Int J Clin Exp Med 2018;11(9):9333-9342
www.ijcem.com /ISSN:1940-5901/IJCEM0072029

Original Article

Antagonization of CCR4 leads to failure of activated regulatory T-cell migration in a mice model of head and neck squamous cell carcinoma

Wei-Jin Li[1,2*], Wei Sun[1*], Fan-Qin Wei[1,3*], Wei-Ping Wen[1]

[1]Department of Otorhinolaryngology Head and Neck Surgery, The First Affiliated Hospital of The Sun Yat-sen University, Guangzhou, China; [2]Department of Otorhinolaryngology Head and Neck Surgery, The Third Affiliated Hospital of The Sun Yat-sen University, Guangzhou, China; [3]Department of Otorhinolaryngology Head and Neck Surgery, The Sixth Affiliated Hospital of The Sun Yat-sen University, Guangzhou, China. [*]Equal contributors.

Received August 26, 2017; Accepted June 4, 2018; Epub September 15, 2018; Published September 30, 2018

Abstract: By mediating immune tolerance in head and neck squamous cell carcinomas (HNSCC), regulatory T-cells (Tregs) are not functionally heterogeneous. Animal models of HNSCC regarding $CD4^+CD45RA^-CD25^{+++}$ Treg cells [activated Treg (aTreg) cells] have not been reported, making it difficult to target tumor-infiltrating aTregs. This present study confirmed that mice aTreg cells, with suppressive capacity, were dramatically increased in the tumor microenvironment. Moreover, C-C chemokine receptor 4 (CCR4) was specifically expressed by aTreg cells while MCP-1 (CCL2), CCL17 (TARC), CCL22 (MDC), and endogenous CCR4-binding ligands were upregulated in the tumor microenvironment. An *in vitro* study showed that aTreg migration was successfully blocked after use of a CCR4 antagonist. Therefore, blocking the recruitment of aTreg cells induced by CCR4 is a promising method for future studies on immunotherapy for HNSCC.

Keywords: CCR4, tumor microenvironment, activated Treg, mouse, head and neck squamous cell carcinoma, antagonist

Introduction

Head and neck squamous cell carcinoma (HNSCC) is the sixth most common type of malignancy, worldwide [1]. Survival rates for this disease have not improved for several decades, despite many efforts made regarding chemotherapy, radiotherapy, and surgery [2].

Failure of antitumor immune activities is highly associated with progression and recurrence of HNSCC [3]. $Foxp3^+CD25^+CD4^+$ regulatory T(Treg) cells play a crucial role in immune tolerance by keeping tumor-specific T-cell responses from fulfilling their task [4, 5].

The frequency and prognostic value of Tregs in different cancers have long been discussed [6-9]. However, studies involving depletion of Treg cells have shown different effects regarding antitumor immune response [10-14], partly due to their varied function. For example, a portion of $CD4^+CD25^+$ T-cells show no capability in antitumor suppression but produce interleukin (IL)-2, which is needed for antitumor responses. Therefore, when targeting all $CD4^+CD25^+$ T-cells, collateral damage might be made [12]. Hence, a new approach is needed to target Treg cell accumulation in the tumor microenvironment instead of depleting the whole $CD25^+$ T-cell subset.

In 2009, Miyara et al. demonstrated that Tregs can be divided into three functionally distinct subsets on the basis of CD45RA, FoxP3, and CD25 expression: resting Tregs (rTreg cells) which are $CD45RA^+Foxp3^{low}CD25^{++}$ Tregs, activated Tregs (aTreg cells) which are $CD45^-Fxop3^{low}CDE25^{++}$ Tregs, and cytokine-secreting non-suppressive T-cells which are $CD45RA^-Foxp3^{low}CD25^+CD4^+$ T-cells [15]. Previous results have shown that, from peripheral blood mononuclear cells (PBMC) of HSNCC patients, a significant increase was found in activated

Tregs (aTreg cells), which are highly suppressive, while a decrease in resting Tregs (rTreg cells) was found [16, 17].

By evaluating markers of chemokine receptors on the surface of tumor-infiltrating Tregs in HNSCC patients, it was found that the C-C chemokine receptor (CCR) 4 was exclusively highly expressed on the surface of peripheral aTregs, while monocyte chemoattractant protein-1 (MCP-1), an endogenous CCR4-binding ligand, was specifically upregulated in the HNSCC microenvironment [18]. However, similar division of Tregs was not reported in HNSCC mice models. Moreover, the mechanisms that mediate recruitment of Tregs within mouse tumor tissues remain unclear. Thus, an experiment of CCR4 antagonist was inappropriate for study, *in vivo*.

This present assessed frequencies of the 3 functionally distinct subsets of $CD4^+CD25^+$ $Foxp3^+$ T-cells in mice with HNSCC. It was confirmed that, in a mice model, distinct subsets of Treg cells have similar variations in function as in humans. Furthermore, CCR4 expression on the 3 subsets of mouse Tregs was investigated, finding that CCR4 was exclusively highly expressed on aTreg cells, while its binding ligands MCP-1 (CCL2), TARC (CCL17), and MDC (CCL22) were upregulated in mice tumor microenvironment. This study evaluated the clinical importance of CCR4 antagonist, *in vitro*, and argued that an *in vivo* experiment on the blockade of aTreg cell trafficking was viable and of great importance.

Materials and methods

Animals and tumor cell lines

Male C3H-HeN mice, 8 weeks old, were purchased from Slac Laboratory Animal Co., Ltd., (Shanghai, China). All mice used for experiments were housed under specific pathogen-free conditions. Procedures performed were approved by the Institutional Animal Studies Committee and conducted in accordance with the Institutional Animal Care and Use Committee (IACUC) guidelines. SCC VII cells, a cell line of mouse OSCC, were kindly provided by West China Hospital.

Antibodies and reagents

All antibodies were purchased from eBioscience (Germany) unless specified otherwise. The following antibodies were used for surface staining: anti-mouse CD3-eFluor 605NC, anti-mouse CD4-eFluor 450, anti-mouse CD-25-APC, anti-mouse CCR4-PE, and anti-mouse CD45RA-FITC from Santa Cruz. Anti-mouse Foxp3-PE and Foxp3 fixation/permeabilization kits were obtained for intracellular staining. Soluble anti-mouse CD3e and CD28 functional grade purified were also used for activation of T-cells *in vitro*. Isotype controls were purchased from the same company.

Preparation of lymphocytes

Single cell suspensions of lymphocytes were prepared by enzymatic digestion [26]. After mice were sacrificed on day 21 and day 28 after tumor injections, tumors and spleens were removed and minced into small pieces with a scalpel. Samples were then immersed in 10 mL of digestion mixture of RPMI 1640 with 5% fetal bovine serum 0.5 mg/mL collagenase A, 0.2 mg/mL hyaluronidase type V, and 0.02 mg/mL DNase I (Sigma-Aldrich St. Louis, MO, USA). After 30 minutes of incubation on a platform at 37°C, samples were filtered through 40-nm cell strainers (BD Biosciences, San Diego, CA, USA). From single cell suspensions obtained above, lymphocytes were then further extracted using Ficoll-Hypaque (Haoyang Bio, Tianjin, China).

Surface and intracellular staining

To identify $Foxp3^+CD4^+$ T-cell subsets, surface and intracellular staining were performed. Antibodies against surface markers CD4, CD25, CD45RA and CCR4 were added to the lymphocyte suspensions and incubated on ice for 45 minutes in the dark. After two washings, cells were fixed and permeabilized with fixation/permebilization buffer for 1 hour on ice in the dark. After washing, intracellular antibodies against Foxp3 were added and incubated for 1 hour in the dark at room temperature. After two additional washings, cells were examined by multicolor flow cytometry. For each sample, proper isotype Ab controls were included.

Multicolor flow cytometry

After labeling with antibodies, single cell suspension was examined twice by multicolor flow cytometry. Percentages of cells stained with particular antibodies were analyzed by a 10-color (3 laser: 488 nm blue, 638 nm red, and

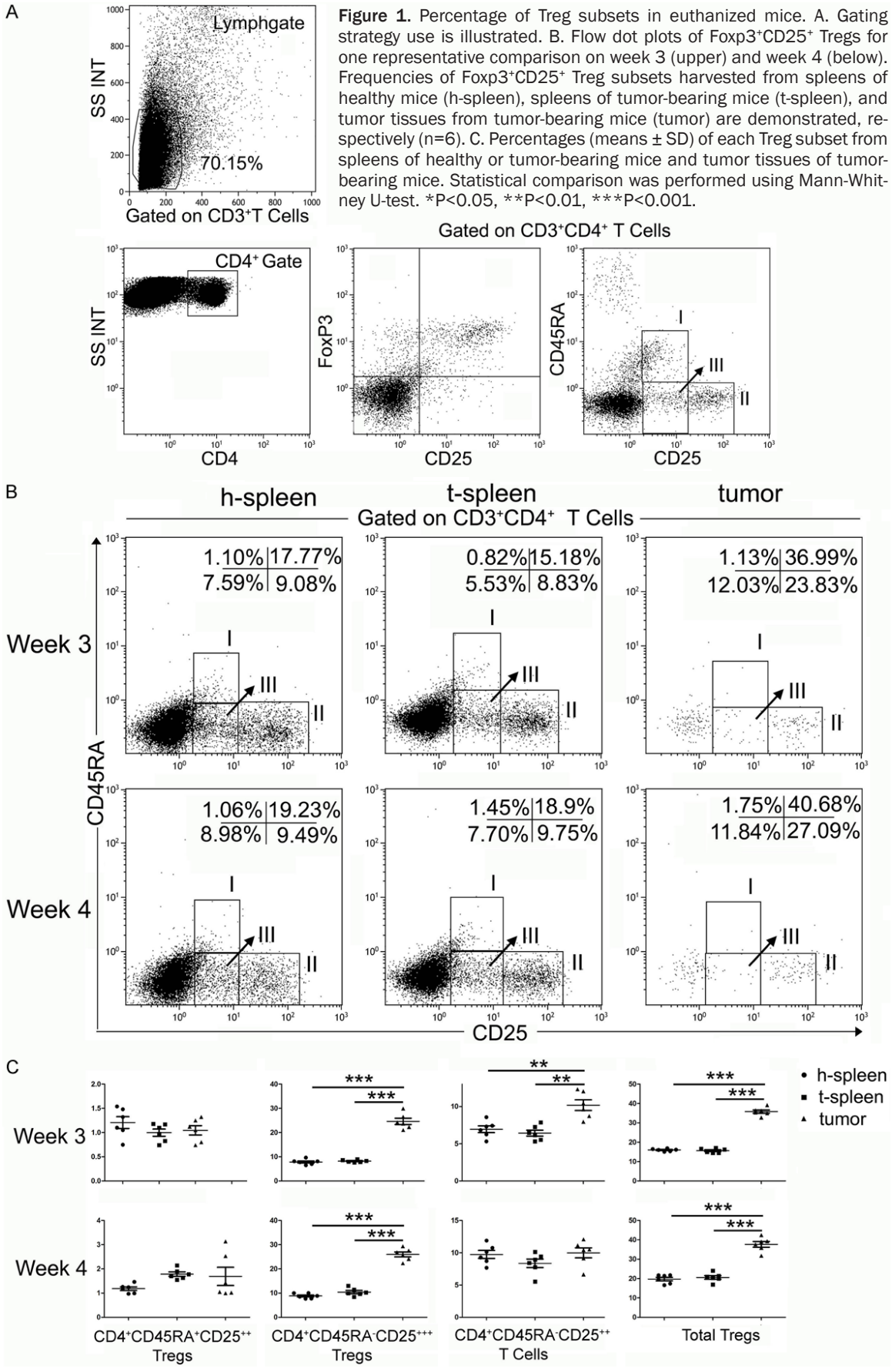

Figure 1. Percentage of Treg subsets in euthanized mice. A. Gating strategy use is illustrated. B. Flow dot plots of Foxp3$^+$CD25$^+$ Tregs for one representative comparison on week 3 (upper) and week 4 (below). Frequencies of Foxp3$^+$CD25$^+$ Treg subsets harvested from spleens of healthy mice (h-spleen), spleens of tumor-bearing mice (t-spleen), and tumor tissues from tumor-bearing mice (tumor) are demonstrated, respectively (n=6). C. Percentages (means ± SD) of each Treg subset from spleens of healthy or tumor-bearing mice and tumor tissues of tumor-bearing mice. Statistical comparison was performed using Mann-Whitney U-test. *P<0.05, **P<0.01, ***P<0.001.

405 nm violet) Gallios Flow Cytometer (Beckman Coulter, Hercules, CA, USA) equipped with Gallios Software v1.0. Gating strategy was performed as described [15].

Cell culture

RPMI 1640 medium supplemented with 10% fetal bovine serum, 100 IU/mL penicillin, and 100 mg/mL streptomycin (Sigma, St. Louis, MO) was used for T-cell culturing. For tumor cell lines, DMEM medium supplemented with 10% fetal bovine serum, 100 IU/mL penicillin, and 100 mg/mL streptomycin (Sigma, St. Louis, MO) was used.

In vitro suppression assay of three distinct Treg subsets

Cells stained with antibodies against CD4, CD25 and CD45RA were adjusted to a concentration of 1×10^4 cells/μl. Using a FACS cell sorter (BD Influx, BD Biosciences), live cells of Treg subsets were sorted out as follows: $CD2525^{++}CD45RA^{+}$ cells as $FoxP3^{low}CD45RA^{+}$ (I), $CD25^{+++}CD45RA^{-}$ cells as $FoxP3^{high}CD45RA^{-}$ (II), and $CD25^{++}CD45RA^{-}CD4^{+}$ T cells as $FoxP3^{low}CD45RA^{-}$ (III), respectively [15].

After sorting, each of the 3 subsets of Treg cells were added with 5×10^3 responder cells (1:1 ratio) labeled with 1 μM carboxyfluorescein diacetate succinimidyl ester (CFSE) (eBioscience, San Diego, CA, USA). Soluble anti-CD28 (2 μg/mL) and plate-bound anti-CD3 (0.5 μg/mL) were used in the co-culture system. After 72 hours of co-culturing, cells were harvested and analyzed by flow cytometry. Percentages of suppression were determined by the proliferation index (PI, frequencies of proliferated cells in each group/frequency of proliferated cells in a responder cell control group X 100%) of a responder cell control group (100% proliferation, 0% suppression), compared with the PI of responder cells co-cultured with each Treg subset.

Migration assay

Migration assay was performed as previously described [27]. 1×10^4 aTreg cells were incubated with a CCR4 antagonist ($C_{27}H_{41}N_5O_2$.2HCL, 0.14 μM, TOCRIS, Minneapolis, MN, USA) for 30 minutes at 37°C. Anti-mouse-CCL2 antibodies (Monoclonal Mouse IgG1 Clone #24822, 15 μg/mL, R & D Systems) or tumor extracts were added to the lower chamber. Migrated cells were counted with an automated cell counter (Scepter, Millipore, Billerica, MA, USA).

Immunohistochemical analysis

Detection of chemokine receptor ligands MCP-1 (CCL2), TARC (CCL17), and MDC (CCL22) antibodies was performed on 4 μm-thick paraffin-embedded sections of tumor tissue and paracancerous tissue samples with indicated antibodies using an ABC kit (PK-4001, ZSGBBIO).

Statistical analysis

Statistical analysis was performed with SPSS Standard version 13.0 software (IBM, Chicago, IL, USA). Differences in frequencies of the total Treg subset between groups were assessed using Student's t-tests, while differences of frequencies of distinct Treg subsets and CCR4 expression on distinct Treg subsets subsets were assessed using Mann-Whitney U-test. Suppressive function of distinct Treg groups and recruiting function of CCR4 on aTreg were analyzed using Kruskal-Wallis tests. Comparison of MCP-1 (CCL2), TARC (CCL17), and MDC (CCL22) expression between tumor tissues and paracancerous tissues was performed using Wilcoxon matched-pairs signed-ranks test. *P*-values less than 0.05 were considered statistically significant.

Results

Total aTreg cells were accumulated in mice HNSCC tissue

Figure 1A demonstrates the gating strategy to identify the whole $CD4^{+}CD25^{+}Foxp3^{+}$ Treg subset. On week 3, the frequency of all $CD4^{+}CD25^{+}Foxp3^{+}$ Tregs from tumor tissues was higher than Tregs from spleens of healthy mice or tumor-bearing mice (35.84±0.86% vs. 16.01±0.28%, P<0.0001; 35.84±0.86% vs. 15.66±0.47%, P<0.0001, respectively), while the latter two did not show any significant differences (16.01±0.28% vs. 15.66±0.47%, P> 0.05). The tendency remained the same on week 4 (37.65±1.47% vs. 19.73±0.93%, P< 0.0001; 37.65±1.47% vs. 20.57±0.94%, P< 0.0001; 19.73±0.93% vs. 20.57±0.94%, P>

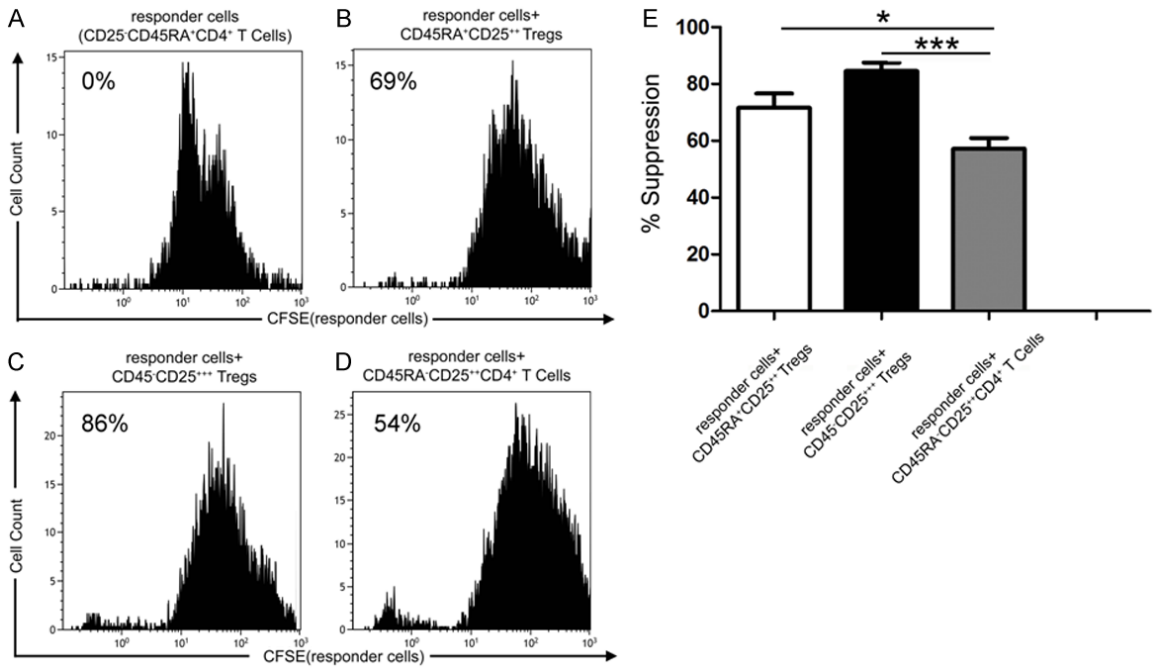

Figure 2. Percentage of suppression by each Treg subset on the proliferation of responder T-cells. A-D. CFSE dilution by 1 × 10^4 labeled $CD4^+CD25^-CD45RA^+$ T-cells (responder T-cells) assessed after 72 hours of TCR-stimulated co-culture with the indicated Treg subset at a 1:1 ratio. Flow plots for one representative tumor-bearing mouse. Percentage of suppression is indicated. E. The histogram represents mean percentage of suppression ± SD (n=5). Statistical comparison was performed using Student's t-test. *P<0.05, ***P<0.001.

0.05, respectively). After 1 week of tumor-glowing, more Treg cells were gathered in spleens of tumor-bearing mice sacrificed on week 4 than that on week 3 (20.57±0.94% vs. 15.66±0.47%, P<0.001). Results showed that, with tumors planted, total Tregs accumulated within the tumor-microenvironment. Further investigation, however, should be done to determine the distribution of the 3 subsets from increased Tregs.

aTreg cells were the major factor of treg cell accumulation in mice HNSCC tissue

After dividing the whole Treg subset into three distinct subsets, frequencies of each subset were assessed from tumor tissues of tumor-bearing mice, spleens of healthy mice(h-spleen), and spleens of tumor-bearing mice (t-spleen) (**Figure 1B**).

On week 3, the frequency of $CD4^+CD45RA^+Foxp3^{low}$ Tregs (rTregs) from t-spleen (0.99±0.07%) was similar to that from h-spleen (1.21±0.12%, P>0.05) or tumor tissues (1.05±0.09%, P>0.05). Frequency of $CD4^+CD45RA^-Foxp3^{low}$ T-cells from t-spleen (6.43±0.40%) was similar to that from h-spleen (6.95±0.45%, P>0.05), but lower than that from tumor tissues (10.18±0.40%, P<0.01). The frequency of $CD4^+CD45RA^-Foxp3^{high}$ Tregs (aTregs) from t-spleen (8.23±0.22%) was higher than that from h-spleen (6.43±0.40%, P<0.01), but lower than the dramatically increased frequency of the same subset from tumor tissues (24.62±1.30%, P<0.0001).

On week 4, the frequency of aTregs from tumor tissues remained much higher than that from h-spleen or t-spleen (25.98±1.02% vs. 8.80±0.42%, P<0.0001; 25.98±1.02% vs. 10.43±0.64%, P<0.0001), while the latter two did not differ from each other (P>0.05).

Moreover, after 1 week of tumor-growing, more aTregs were recruited to tumor tissues on week 4 than on week 3 (25.98±1.02% vs. 24.62±1.30%, P>0.05), yet statistical significance was not reached.

aTreg cells had better suppressive function

Tregs were obtained from tumor tissues of 6 randomly selected mice after 28 days of tumor-bearing and sorted into three distinct Treg subsets. Each subset was co-cultured with

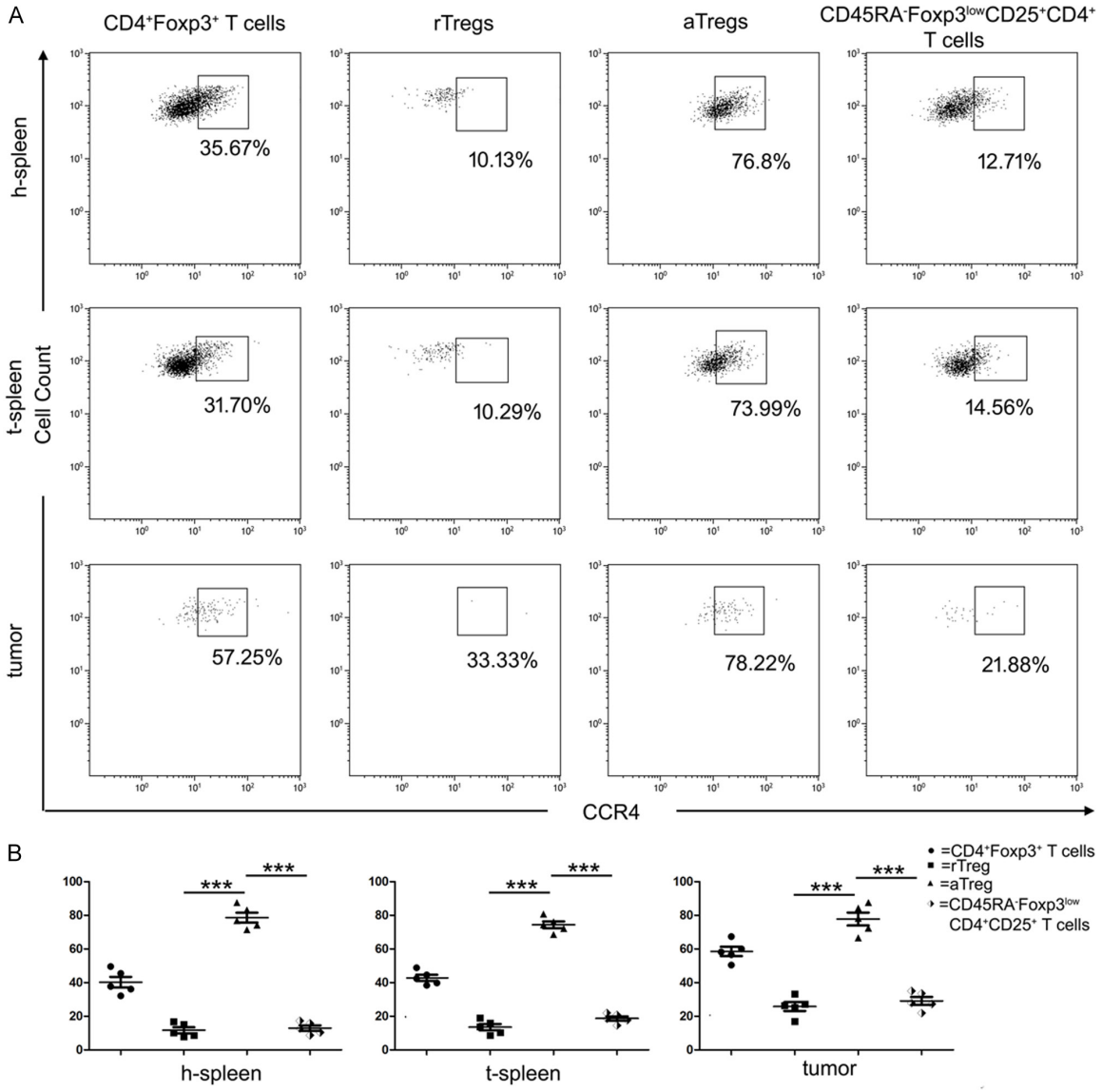

Figure 3. Percentage of CCR4 expression on each Treg subset. A. Flow dot plots of CCR4 expressed on each Treg subset are demonstrated. $CD4^+CD25^+Foxp3^+$ Tregs harvested from h-spleen (spleens of health mice), t-spleen (spleens of tumor-bearing mice), and tumor tissues from tumor-bearing mice are shown respectively. B. Percentages (means ± SD) of CCR4 expression on each Treg subset are demonstrated. Statistical comparisons were performed using Student's t-test. ***P<0.001.

autologous $CD25^-CD45RA^+CD4^+$ responder cells (**Figure 2A-D**). After 72 hours of co-culturing, $CD45RA^+CD25^{++}$ Tregs showed a higher suppression rate compared with $CD45RA^-CD25^+$ Tregs, but differences were not significant (71.67±4.96% vs. 84.50%±3.05%, P>0.05). These 2 subsets both induced a higher suppression rate to $CD45RA^-CD25^{++}CD4^+$ T-cells (71.67±4.96% vs. 57.15±3.79%, P<0.05; 84.50%±3.05% vs. 57.15±3.79%, P<0.001, **Figure 2E**). Mice $CD45RA^-CD25^{++}CD4^+$ T-cells had better suppressive function compared with the same subset assessed from HNSCC patients [17], in accordance with a previous study [19].

CCR4 was predominantly expressed on aTreg cells

To evaluate the importance of CCR4 in recruiting aTreg cells to the mice tumor microenvironment in HNSCC, expression of CCR4 was assessed in Treg cells from h-spleen, t-spleen, and tumor-tissues (n=5) (**Figure 3**). It was found that among all $CD4^+CD25^+Foxp3^+$ Treg cells, Treg cells from tumor tissues (60.42±2.77%)

had a significantly higher CCR4 expression than Treg cells from t-spleen (40.29±4.34%, P< 0.001) or h-spleen (41.19±3.00%, P<0.001).

After dividing $CD4^+CD25^+Foxp3^+$ Treg cells into three distinct subsets, results showed that from the h-spleen group, aTreg cells (78.64± 2.94%) expressed CCR4 on a higher level than rTreg cells (11.70±1.78%, P<0.001%) and $CD45RA^-CD25^{++}CD4^+$ T-cells (12.98±1.60%, P< 0.001%). From the t-spleen group, aTreg cells (74.37±0.04%) expressed CCR4 on a higher level than rTreg cells (13.51±1.86%, P<0.001%) and $CD45RA^-CD25^{++}CD4^+$ T-cells (18.70±1.28%, P<0.0001%). From tumor tissues, aTreg cells (77.82±3.84%) expressed CCR4 on a higher level than rTreg cells (25.77± 2.64%, P<0.001%) and $CD45RA^-CD25^{++}CD4^+$ T-cells (29.11±2.36%, P<0.001%).

Moreover, aTreg cells from tumor tissues expressed CCR4 on a similar level as aTreg cells from h-spleens and t-spleens (77.82± 3.84% vs. 78.64±2.94%, P>0.05; 77.82±3.84% vs. 74.37±0.04%, P>0.05).

The results showed that aTregs from different origins have a dramatically higher CCR4 expression, suggesting that CCR might be a key factor for accumulation of aTregs in the tumor microenvironment.

Tumor tissues had higher expression of CCR4-binding ligands

CCR4 is a receptor for monocyte chemoattractant protein-1 (MCP-1)/CCL2, thymus and activation regulated chemokine (TARC)/CCL-17, and macrophage-derived chemokine (MDC)/CCL22. To confirm expression of these endogenous CCR4-binding ligands in the HNSCC microenvironment, immunohistochemical analysis was used to assess expression of these chemokine ligands in paired tumor and paracancerous tissues from 5 HNSCC tumor-bearing mice (**Figure 4A**). Interestingly, CCL2, CCL17, and CCL22 were all increased in tumor tissues compared with paracancerous tissues (215.6±22.27 vs. 21.80± 9.731, P<0.001; 275.6±25.08 vs. 30.92± 14.02, P<0.001; 271.5±37.46 vs. 26.81±10.94, P<0.001 (**Figure 4B**). Immunohistochemistry results were consistent with the postulation that mouse aTreg cells could be recruited to the tumor microenvironment by ligands through binding to CCR4.

CCR4 antagonist inhibited the recruitment of aTreg cells

The ability of CCR4 to recruit mouse aTreg cells to tumor-tissues was evaluated (**Figure 4C**). Based on a study on migration of aTreg cells from HNSCC patients, MCP-1 (CCL2) was chosen to demonstrate the hypothesis. Freshly sorted aTreg cells from tumor tissues were analyzed in migration assays (n=3). Results showed that tumor extracts and MCP-1 (CCL2) induced significant migration of aTreg cells (P< 0.01 vs. control [medium]; P<0.01 vs. control [medium]). Using a monoclonal antibody against mice MCP-1 (CCL2) and a CCR4 antagonist, migration of aTreg cells was severely blocked, even if induced by tumor extracts of MCP-1 (CCL2) (P<0.01 for each; P<0.01 for each). These results suggest that blocking CCR4-induced-pathways by addressing CCR4 antagonist may result in the inhibition of Treg recruitment.

Discussion

Previous studies have shown that aTreg cells are increased in the peripheral circulation in HNSCC patients and that accumulation of aTreg cells in HNSCC tumor tissues may accelerate disease progression and predict poor survival [16-18]. Therefore, it is of great value to block Treg cell recruitment into the tumor microenvironment. This study aimed to demonstrate the feasibility of this strategy with HNSCC mice.

CD25 and CD45RA were used as two markers to classify Tregs into three distinct subsets. Mouse $CD45RA^-CD25^{++}CD4^+$ T-cells showed a higher suppression rate compared to the same Treg subset in humans, which was in accordance with previous study. However, $CD45RA^-CD25^{+++}$ Tregs had significantly higher suppression rates [19]. No previous studies have reported this classification of mouse Treg cells.

After existence of the classification was confirmed, the distribution of three distinct Treg subsets was assessed in HNSCC mice. Frequencies of aTreg cells from splenocytes were similar between healthy and tumor-bearing mice, contrary to the findings on increasing frequency of aTreg cells in peripheral circulation of HNSCC patients. aTreg cells were dramatically accumulated within tumor tissues and consisted of the majority of tumor-infiltrating Treg cells. This was parallel with an earlier finding in

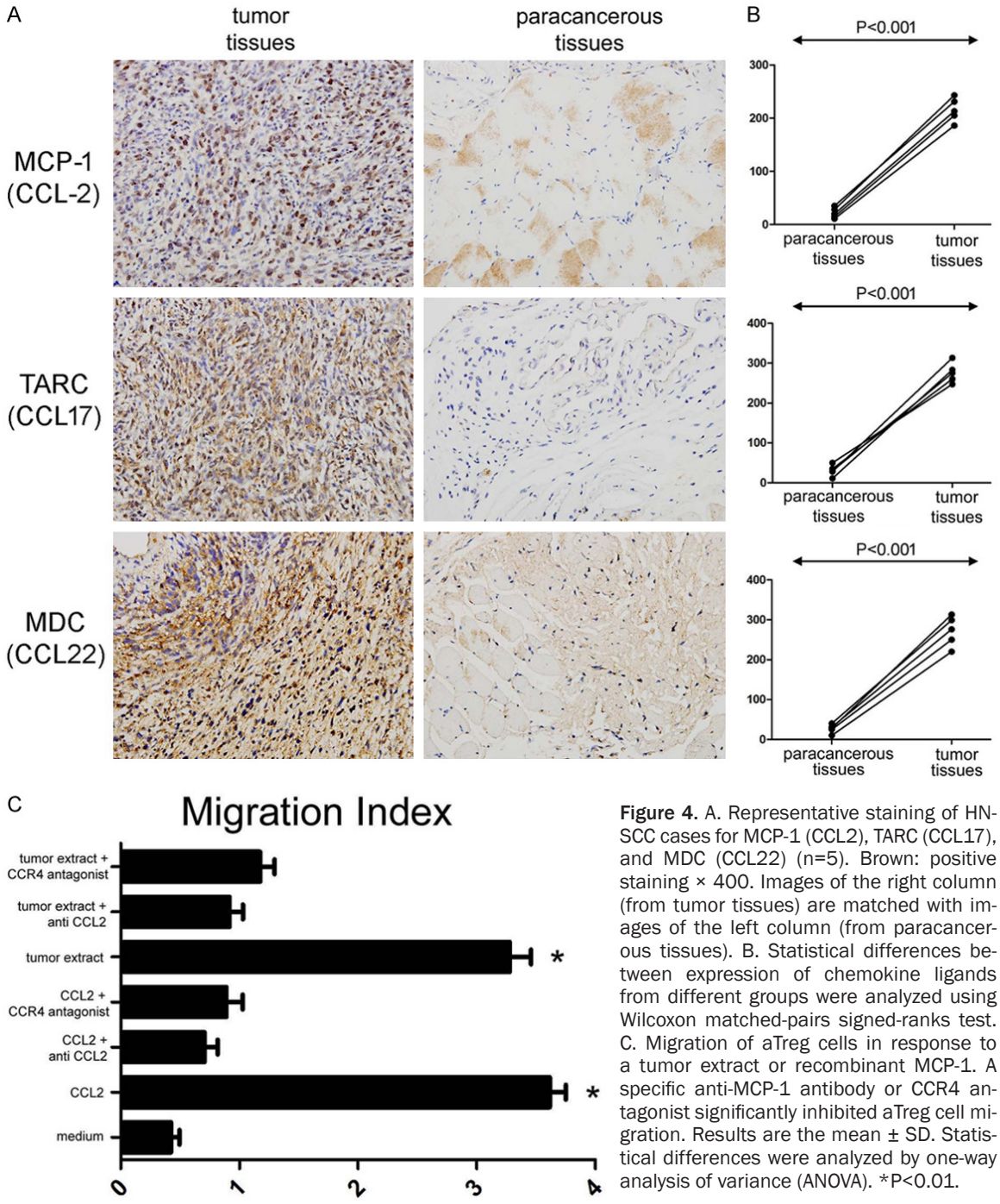

Figure 4. A. Representative staining of HNSCC cases for MCP-1 (CCL2), TARC (CCL17), and MDC (CCL22) (n=5). Brown: positive staining × 400. Images of the right column (from tumor tissues) are matched with images of the left column (from paracancerous tissues). B. Statistical differences between expression of chemokine ligands from different groups were analyzed using Wilcoxon matched-pairs signed-ranks test. C. Migration of aTreg cells in response to a tumor extract or recombinant MCP-1. A specific anti-MCP-1 antibody or CCR4 antagonist significantly inhibited aTreg cell migration. Results are the mean ± SD. Statistical differences were analyzed by one-way analysis of variance (ANOVA). *P<0.01.

HNSCC patients [16-18]. Given the distribution of Treg subsets, it is of great value to inhibit highly suppressive aTreg cells from recruitment to HNSCC tumor microenvironment.

Chemokine receptors have been reported to play a critical role in recruiting immunoregulatory cells [12, 20-23]. Previous work has shown that aTreg cells predominantly express CCR4 compared with $CD4^{+}Foxp3^{+/-}$ T-cells and other immune cells [18]. Based on the many similarities aTreg cells share between mice and humans, it is reasonable to assume that mouse aTreg cells also predominantly express CCR4. To verify this theory, CCR4 expression was assessed in different Treg subsets. The data showed that CCR4 was predominantly expressed in aTreg cells from various origins,

showing that high expression of CCR4 is a unique characteristic for mice aTreg cells.

Moreover, data showed that MCP-1 (CCL2), TARC (CCL17), and MDC (CCL22), all chemoattractant ligands for CCR4, were highly expressed in HNSCC tumor tissues compared with adjacent nontumor tissues. These results strongly suggest that interaction between CCR4 and its ligands plays a vital role in the recruitment of mouse aTreg cells towards the tumor microenvironment.

In addition, the *in vitro* experiment showed that by using a CCR4 antagonist, aTreg migration capacity was largely exhibited. While some earlier studies demonstrated that anti-human CCR4 monoclonal antibodies can enhance antitumor immune response in cancer patients, this study is the first to report that use of a CCR4 antagonist exhibits mice aTreg cell migration without depleting any fragment of $CD25^+$ T-cells in peripheral circulation, possibly explaining the clinical failure and eruption of autoimmunity of CD25 depleting strategy in some studies [24, 25].

In conclusion, this present study suggests that mouse aTreg cells predominantly express CCR4 and that CCR4 antagonists can block migration of mouse aTreg cells. Therefore, future studies should focus on the use of CCR4 antagonists, *in vivo*, which may result in the exhibition of tumor growth and longer mouse survival.

Acknowledgements

This study was supported by The National Natural Science Foundation of China (81602-365) and The National Natural Science Foundation of Guangdong Province (2017A03-0313700).

Disclosure of conflict of interest

None.

Address correspondence to: Dr. Wei-Ping Wen, Department of Otorhinolaryngology Head and Neck Surgery, The First Affiliated Hospital of The Sun Yat-Sen University, 58 Zhongshan Road II, Guangzhou 510080, China. Tel: +86-20-13538885840; E-mail: wenwp@mail.sysu.edu.cn

References

[1] Parkin DM, Bray F, Ferlay J and Pisani P. Global cancer statistics, 2002. CA Cancer J Clin 2005; 55: 74-108.

[2] Forastiere A, Koch W, Trotti A and Sidransky D. Head and neck cancer. N Engl J Med 2001; 345: 1890-1990.

[3] Alhamarneh O, Amarnath SM, Stafford ND and Greenman J. Regulatory T cells: what role do they play in antitumor immunity in patients with head and neck cancer? Head Neck 2008; 30: 251-261.

[4] Khazaie K and von Boehmer H. The impact of $CD4^+CD25^+$ Treg on tumor specific $CD8^+$ T cell cytotoxicity and cancer. Sermin Cancer Biol 2006; 16: 124-136.

[5] Zou W. Regulatory T cells, tumor immunity and immunotherapy. Nat Rev Immunol 2006; 6: 295-307.

[6] Ma R, Jiang T and Kang X. Circulating microRNAs in cancer: origin, function and application. J Exp Clin Cancer Res 2012; 31: 38.

[7] Kobayashi N, Hiraoka N, Yamagami W, Ojima H, Kanai Y, Kosuge T, Nakajima A and Hirohashi S. $FOXP3^+$ regulatory T cells affect the development and progression of hepatorcarcinogenesis. Clin Cancer Res 2007; 13: 902-911.

[8] Chen Y, Zhang Y, Liao W, Zhou J, He G, Xie X, Fei R, Qin L, Wei L and Chen H. FOXP3 gene polymorphism is associated with hepatitis B-related hepatocellular carcinoma in China. J Exp Clin Cancer Res 2013; 32: 39.

[9] Okita R, Saeki, Takashima S, Yamaguchi Y and Toge T. $CD4^+CD25^+$ regulatory T cells in the peripheral blood of patients with breast cancer and nonsmall cell lung cancer. Oncol Rep 2005; 14: 1269-1273.

[10] Dannull J, Su Z, Rizzieri D, Yang BK, Coleman D, Yancey D, Zhang A, Dahm P, Chao N, Gilboa E and Vieweg J. Enhancement of vaccine-mediated antitumor immunity in cancer patients after depletion of regulatory T cells. J Clin Invest 2005; 115: 3623-3633.

[11] Attia P, Maker AV, Haworth LR, Rogers-Freezer L and Rosenberg SA. Inability of a fusion protein of IL-2 and diphtheria toxin (Denileukin Diftitox, DAB389IL-2, ONTAK) to eliminate regulatory T lymphocytes in patients with melanoma. J Immunother 2005; 28: 582-592.

[12] Nishikawa H and Sakaguchi S. Regulatory T cells in tumor immunity. Int J Cancer 2010; 127: 759-767.

[13] Litzinger MT, Fernando R, Curiel TJ, Grosenbach DW, Schlom J and Palena C. IL-2 immunotoxin denileukin diftitox reduces regulatory T cells and enhances vaccine-mediated T-cell immunity. Blood 2007; 110: 3192-3201.

[14] Rech AJ, Mick R, Martin S, Recio A, Aqui NA, Powell DJ Jr, Colligon TA, Trosko JA, Leinbach LI, Pletcher CH, Tweed CK, DeMichele A, Fox KR, Domchek SM, Riley JL and Vonderheide RH. CD25 blockade depletes and selectively reprograms regulatory T cells in concert with immunotherapy in cancer patients. Sci Transl Med 2012; 4: 134-162.

[15] Miyara M, Yoshioka Y, Kitoh A, Shima T, Wing K, Niwa A, Parizot C, Taflin C, Heike T, Valeyre D, Mathian A, Nakahata T, Yamaguchi T, Nomura T, Ono M, Amoura Z, Gorochov G and Sakaguchi S. Functional delineation and differentiation dynamics of human $CD4^+$ T cells expressing the Foxp3 transcription factor. Immunity 2009; 30: 899-911.

[16] Sun W, Li WJ, Wu CY, Zhong H and Wen WP. $CD45RAFoxp3^{high}$ but not $CD45RA^+Foxp3^{low}$ suppressive T regulatory cells increased in the peripheral circulation of patients with head and neck squamous cell carcinoma and correlated with tumor progression. J Exp Clin Cancer Res 2014; 33: 35.

[17] Sun W, Li WJ, Fu QL, Wu CY, Lin JZ, Zhu XL, Hou WJ, Wei Y, Wen YH, Wang YJ and Wen WP. Functionally distinct subsets of $CD4^+$ regulatory T cells in patients with laryngeal squamous cell carcinoma are indicative of immune deregulation and disease progression. Oncol Rep 2015; 33: 354-362.

[18] Sun W, Li WJ, Wei FQ, Wong TS, Lei WB, Zhu XL, Li J and Wen WP. Blockade of MCP-1/CCR4 signaling-induced recruitment of activated regulatory cells evokes an antitumor immune response in head and neck squamous cell carcinoma. Oncotarget 2016; 7: 37714-37727.

[19] Baecher-Allan CM and Hafler DA. Functional analysis of highly defined FACS-isolated populations of human regulatory $CD4^+CD25^+$ T cells. Clin Immunol 2005; 117: 192.

[20] Curiel TJ, Coukos G, Zou L, Alvarez X, Cheng P, Mottram P, Evdemon-Hogan M, Conejo-Garcia JR, Zhang L, Burow M, Zhu Y, Wei S, Kryczek I, Daniel B, Gordon A, Myers L, Lackner A, Disis ML, Knutson KL, Chen L and Zou W. Specific recruitment of regulatory T cells in ovarian carcinoma fosters immune privilege and predicts reduced survival. Nat Med 2004; 10: 942-949.

[21] Parsonage G, Machado LR, Hui JW, McLarnon A, Schmaler T, Balasothy M, To KF, Vlantis AC, van Hasselt CA, Lo KW, Wong WL, Hui EP, Chan AT and Lee SP. CXCR6 and CCR5 localize T lymphocyte subsets in nasopharyngeal carcinoma. Am J Pathol 2012; 180: 1215-1222.

[22] Zou W, Machelon V, Coulomb-L'Hermin A, Borvak J, Nome F, Isaeva T, Wei S, Krzysiek R, Durand-Gasselin I, Gordon A, Pustilnik T, Curiel DT, Galanaud P, Capron F, Emilie D and Curiel J. Stromal-derived factor-1 in human tumors recruits and alters the function of plasmacytoid precursor dendritic cells. Nat Med 2001; 7: 1339-1346.

[23] Iellem A, Mariani M, Lang R, Recalde H, Panina-Bordignon P, Sinigaglia F and D'Ambrosio D. Unique chemotactic response profile and specific expression of chemokine receptors CCR4 and CCR8 by CD4(+)CD25(+) regulatory T cells. J Exp Med 2001; 194: 847-853.

[24] Kurose K, Ohue Y, Wada H, Iida S, Ishida T, Kojima T, Doi T, Suzuki S, Isobe M, Funakoshi T, Kakimi K, Nishikawa H, Udono H, Oka M, Ueda R and Nakayam E. Phase Ia study of $FoxP3^+$ CD4 Treg depletion by infusion of a humanized Anti-CCR4 antibody, KW-0761, in cancer patients. Clin Cancer Res 2015; 21: 4327-4336.

[25] Duvic M, Pinter-Brown LC, Foss FM, Sokol L, Jorgensen JL, Challagundla P, Dwyer KM, Zhang X, Kurman MR, Ballerini R, Liu L and Kim YH. Phase 1/2 study of mogamulizumab, a defucosylated anti-CCR4 antibody, in previously treated patients with cutaneous T-cell lymphoma. Blood 2015; 125: 1883-1889.

[26] Lee H, Lee H, Kwon Y, Lee JH, Kim J, Shin MK, Kim SH and Bae H. Methyl gallate exhibits potent antitumor activities by inhibiting tumor infiltration of $CD4^+CD25^+$ regulatory T cells. J Immunol 2010; 185: 6698-6705.

[27] Parsonage G, Machado LR, Hui JW, McLarnon A, Schmaler T, Balasothy M, To KF, Vlantis AC, van Hasselt CA, Lo KW, Wong WL, Hui EP, Chan AT and Lee SP. CXCR6 and CCR5 localize T lymphocyte subsets in nasopharyngeal carcinoma. Am J Pathol 2012; 180: 1215-1222.